



Research Paper

Experimental investigation and effectiveness analysis of a desiccant wheel dehumidification system with low air humidity



Zhiyao Ma, Xiaohua Liu, Tao Zhang*

Department of Building Science and Technology, Tsinghua University, Beijing 100084, China

ARTICLE INFO

Keywords:

Rotary desiccant wheel
Deep dehumidification
Thermodynamic effectiveness
Energy efficiency
Surplus temperature rise
Experimental investigation

ABSTRACT

The desiccant wheel dehumidification system is a feasible approach to realize the deep-dehumidification process to produce supply air with dew point temperature below 0 °C in modern architecture fields. However, actual dehumidification performance of the desiccant wheel system under low humidity condition and its difference from normal humidity dehumidification process have not been experimentally demonstrated. This study, therefore, carried out experiments to investigate the dehumidification performance as well as the thermodynamic effectiveness of the desiccant wheel deep dehumidification system. The results reveal that the desiccant wheel dehumidification system show relatively higher relative dehumidification capacity under low inlet process air conditions, reaching 77.4% under the regeneration air state of 75 °C and 4 g/kg by supplying air humidity under 1 g/kg. The sensitivity of dehumidification performance varying with regeneration humidity is reduced when the desiccant wheel is operated at high regeneration temperature. The deep dehumidification process also shows much greater isenthalpic deviation and surplus temperature deviation than normal dehumidification process due to larger irreversible heat loss, and the thermodynamic effectiveness is also highly related to the regeneration parameters. The study provides theoretical and experimental reference for the effective and efficient design of the desiccant wheel assisted deep dehumidification system.

1. Introduction

Modern architecture fields such as pharmaceutical factories [1], food storage [2], ice arenas [3], and electronic factories [4] often have a demand for deep-dehumidification process. Air humidity is a key parameter for these occasions, and it is usually required to be supplied with dew point temperature below 0 °C. Different from typical residential and commercial buildings, the heating, ventilation and air-conditioning (HVAC) system often accounts for 24%-75% of the total energy use in these fields, among which the dehumidification system is considered one of the main energy-consuming processes [1,5-7]. Hence, it is essential for energy efficiency improvement of the dehumidification system in these deep-dehumidification required fields.

The desiccant wheel system has been widely used as an alternative to the conventional cooling system for air dehumidification and conditioning in modern industries [8-11]. As the desiccant wheel rotates constantly across the process and regeneration air streams, the solid desiccant periodically adsorbs moisture from the process air and desorbs it to the regeneration air. At the same time, latent heat and mass transfer happens with the moisture adsorption and desorption process. The

moisture is removed from the process air to produce dry air for the required environment as a result. Multiple researchers have been conducted to investigate the cooling and dehumidification performance of the desiccant wheel dehumidification system in recent years. La et al. [12] reviewed the recent developments in desiccant wheel cooling system and concluded that the researches mainly focus on terms of desiccant material, mathematical model and system configuration. Yamaguchi and Saito [13] conducted numerical and experimental measurements to analyze the system performance of rotary desiccant wheels. The research clarified the effect of different parameters including regeneration air temperature, air superficial velocity and wheel thickness on the system performance, and the air humidity ratio could be processed from 19.5 g/kg to 9 ~ 16 g/kg with the variation of operating parameters. Zendehboudi and Esmaeili [14] investigated the supply and regeneration area ratio on the performance of desiccant wheels in hot and humid climates to produce air at humidity ratio of 7.5–13.5 g/kg. Saputra et al. [15] carried out experiments to investigate the dehumidification performance of the desiccant wheel for changes in regeneration heat input under an inlet humidity ratio of 15 g/kg and total dehumidification capacity of 3.8–7.0 g/kg. Tu et al. [16] analyzed the effect of the number of stages on the regeneration temperature of

* Corresponding author.

E-mail address: zt2015@mail.tsinghua.edu.cn (T. Zhang).

Nomenclature	
Variables	
c_p	specific heat capacity [kJ/(kg·K)]
COP	coefficient of performance (dimensionless)
$DCOP$	dehumidification coefficient of performance (dimensionless)
h	enthalpy (kJ/kg)
$HVAC$	heating, ventilation and air-conditioning
m	flowrate (m^3/s)
q	thermal consumption (kW)
r	latent heat of vaporization of moisture (kJ/kg)
RDC	relative dehumidification capacity (dimensionless)
t	temperature ($^\circ\text{C}$)
W_{max}	maximum water content of the desiccant material
<i>Subscripts</i>	
a	air
amb	ambient
in	inlet
out	outlet
p	process air
r	regeneration air

Table 1

Recent studies on the deep dehumidification performance of desiccant dehumidification systems.

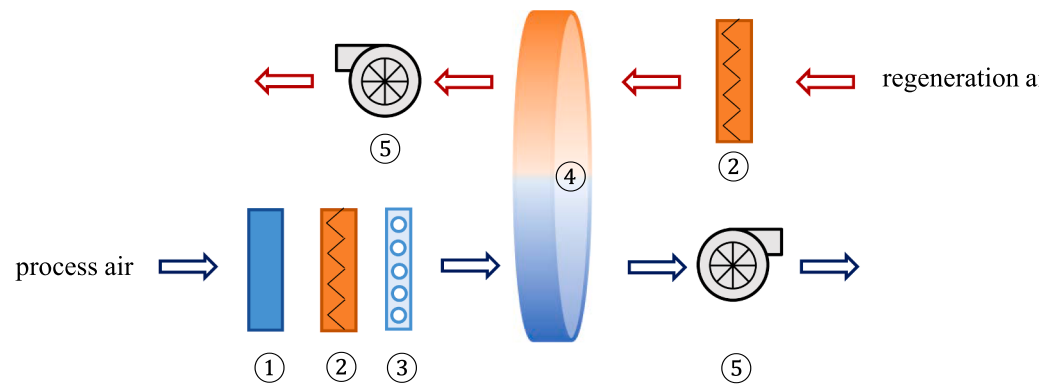
Authors	Fields	Methods	Inlet process air states	Outlet process air states	Regeneration air states	COP_e	$DCOP$	Desiccant wheel
Mahmood et al. [28]	Fruit storage	Experiment	19–37 °C 10–22 g/kg	14–22 °C 3–12.5 g/kg	50–80 °C	/	/	Polymeric
Ahmed et al. [29]	Battery manufacturing plant	Numerical simulation	10 °C 6.8 g/kg	12 °C 0.15 g/kg	146 °C	3.5	/	/
Guan et al. [30]	Battery manufacturing plant	On-site measurement	~12.0 °C 7.4 g/kg	~27.4 °C 2.6 g/kg	~103 °C 19.4 g/kg	0.65–0.68	/	Silica gel
Chen et al. [31]	Multiple deep dehumidification fields	Numerical simulation	–12.5 °C 1.0 g/kg	–10 °C 0.2 g/kg	60 °C, 10.0 g/kg; 75 °C, 15.6 g/kg	2.7	/	Silica gel
Guan et al. [32]	Curling arena	On-site measurement	~15 °C 4.3 g/kg	~3 °C 0.4 g/kg	~73 °C 4.3 g/kg	/	0.50–0.57	Silica gel

desiccant wheel and mentioned that 2 to 4 stages of desiccant wheel showed optimum energy efficiency under normal dehumidification depth. Ge et al. [17] also analyzed the system performance of a two-stage desiccant wheel cooling system under different regeneration temperatures of 50–90 °C. The cascading two-stage desiccant wheel could process the ambient air from 14.3 g/kg to an average of 6.3 g/kg. The results revealed that the cooling power of the system increases but the thermal COP decreases with the increase of regeneration temperature. Liu et al. [18] developed a two-stage desiccant wheel system regenerated by a photovoltaic power generation device and solar thermal collector applied for low latitude isolated islands. The study indicated that the system dehumidification capacity would increase by 0.9–2.7 g/kg for regeneration temperature rising by every 10 °C. Ruivo and Angrisani [19] proposed a pair of effective parameters to evaluate the dehumidification behavior of the desiccant wheel. The experimental results showed that the desiccant wheel had the isenthalpic deviation of 0.05–0.41 and the relative humidity effectiveness of 0.75–1.1 when the inlet process air temperature ranged from 22.2 to 38.8 °C and humidity ratio varied between 6.4 and 15.9 g/kg.

The energy performance of the desiccant dehumidification system has also been studied in the past few years. Angrisani et al. [20] assessed the energy performance of a hybrid desiccant cooling system to process air from 32 °C, 13 g/kg to 20 °C, 9 g/kg. The proposed system showed higher or at least equal thermal and electrical energy efficiency with emissions reductions up to 34% compared with other air-conditioning technologies. Gadalla and Saghafifar [21] proposed multiple cooling systems using the multi-stage desiccant wheel and the proposed system showed better energy performance compared to the conventional cooling system. Caliskan et al. [22] developed a novel air-cooling system consisting of the desiccant wheel and the evaporative cooler to process air at 8.04 g/kg with enhanced energy efficiency. The desiccant wheel

integrated with the solar system was also proposed and investigated by several researchers [23–25]. The solar-driven desiccant cooling system showed less energy consumption compared with the conventional vapor compression system for dehumidification in commercial buildings [23]. However, most of the existing studies were carried out within the humidity range of typical comfortable air conditions, and the investigation of effectiveness of dehumidification as well as the energy performance of the desiccant wheel producing air with low humidity was still insufficient.

For the mentioned applications requiring deep dehumidification, the conventional refrigeration cooling system providing chilled water is usually unable to meet the demand humidity of air process. The desiccant wheel is a feasible method to realize the dehumidification process to supply air with dew point temperature below 0 °C [26,27], and it has been commercially adopted for the fields such as lithium battery factories for many years. Some researchers have investigated the performance of desiccant dehumidification systems applied to the environment requiring low air humidity, and the results were summarized in Table 1. Mahmood et al. [28] evaluated the energy efficiency of desiccant wheel dehumidification applied in the storage of dried fruits. The system could effectively treat outdoor air to the minimum humidity ratio of 3 g/kg. Ahmed et al. [29] applied the desiccant wheel system to dehumidify the process air to 0.15 g/kg in a battery manufacturing plant, and the desiccant wheel was regenerated by passing the air stream heated to 146 °C. Guan et al. [30] investigated the actual performance of a deep-dehumidification system in a lithium battery manufacturing plant. The system consisted of multiple cooling coils and a desiccant wheel, and the results indicated that the system could achieve the outlet humidity ratio of around 2.6 g/kg with an average system COP between 0.65 and 0.68. Chen et al. [31] proposed a dehumidification process with cascading desiccant wheels to produce dehumidified air with a



(1) evaporator; (2) electric heater; (3) electric dehumidifier; (4) desiccant wheel; and (5) fan

(a)



(b)

Fig. 1. Configuration of the experimental system: (a) Schematic diagram, and (b) Photographic view of the experimental system.

Table 2
Summary of basic experimental conditions.

Number	Process air			Regeneration air		
	$t_{p,in}$ (°C)	$\omega_{p,in}$ (g/ kg)	m_p (m ³ / h)	$t_{r,in}$ (°C)	$\omega_{r,in}$ (g/ kg)	m_r (m ³ / h)
1	6	4	6000	75	4	2000
2	6	4	6000	90	4	2000
3	6	4	6000	105	4	2000
4	6	4	6000	75	24	2000
5	6	4	6000	90	24	2000
6	6	4	6000	105	24	2000
7	13	9	6000	75	4	2000
8	13	9	6000	90	4	2000
9	13	9	6000	105	4	2000
10	13	9	6000	75	24	2000
11	13	9	6000	90	24	2000
12	13	9	6000	105	24	2000
13	6	4	4500	75	4	1500
14	6	4	4500	90	4	1500
15	6	4	4500	105	4	1500

dew-point temperature of -30°C from a dry bulb temperature of -12.5°C while exhibiting fewer electricity and heat inputs. Guan et al. [32] carried out on-site measurements and numerical simulation on a desiccant wheel dehumidification system supplying air humidity ratio below 2.8 g/kg in a curling area for the 2022 Winter Olympics, and the results revealed that the system could achieve thermal COP of 0.50–0.57 when using the low-temperature and low-humidity outdoor air as the regeneration. However, the above research mainly focused on the specific operation status and the overall energy consumption of the deep dehumidification system based on on-site measurement and numerical simulation, and there was still a lack of detailed experimental analysis on the actual performance of the desiccant wheel corresponding to the deep dehumidification process.

Based on previous research, there are still limited studies that have investigated the actual performance of desiccant wheel under low humidity dehumidification process, and the differences in dehumidification performance between normal humidity and low humidity dehumidification are not clearly demonstrated. This study, therefore, carried out experiments to investigate the system performance of desiccant wheel dehumidification system with low air humidity. The dehumidification efficiency and the thermodynamic effectiveness of the desiccant wheel deep dehumidification process are analyzed. Based on the conception of isenthalpic deviation, a brand effectiveness parameter, the surplus temperature rise, is also introduced and analyzed in the study. The major differences in dehumidification parameter sensitivity and the thermodynamic effectiveness between normal dehumidification and deep dehumidification are further discussed. The study can provide a reference for the effective and efficient design of the deep dehumidification system in these applications.

2. Methods

2.1. System description and setup conditions

The configuration of the desiccant wheel dehumidification system is shown in Fig. 1. The experimental system consisted of a desiccant wheel, multiple temperature and humidity control devices, multiple temperature and humidity measurement devices, and two driving fans, as seen in Fig. 1(a). On the process side, the process air at ambient air conditions successively passed through an evaporator, an electric heater, and an electric humidifier to meet the required inlet temperature and humidity ratio. The humid process air then entered the dehumidification section of the desiccant wheel, and the desiccant wheel rotated constantly as it dehumidifies the incoming process air. On the regeneration side, the regeneration air was mixed with the exhaust air and the ambient air to

Table 3
Instrumentation descriptions.

Instrumentations	Parameters	Range	Accuracy
Temperature meter (TJHY WWSZY-1)	Air temperature	-40–100 °C	±0.3 °C
Humidity meter (TJHY WWSZY-1)	Air relative humidity	0–99%	±2%
Dew point meter (DM70)	Air dew point temperature	-50–60 °C	±2°C
Anemometer (WFWZY-1)	Airflow velocity	0.05–30 m/s	±5%

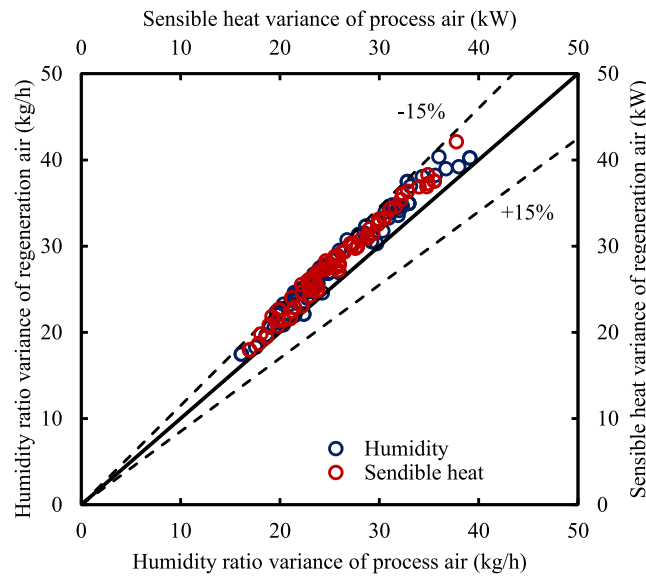


Fig. 2. Sensible heat and mass balances of the experimental results.

meet the required humidity ratio and heated by the electric heater to the required regeneration temperature. Then the regeneration air entered the regeneration section of the desiccant wheel to remove the moisture from the desiccant. The dampers were installed on both the process side and regeneration side to control the constant volumetric airflow rate. The desiccant wheel had a diameter of 0.8 m and a thickness of 0.2 m. The core honeycomb was made of the metal of Aluminum and the desiccant coating on the honeycomb is silica gel. The rotation speed of the desiccant wheel could vary from 1 to 30 r/h. The designed area ratio of process air to regeneration air in the desiccant was 3, and the airflow rate could range from 0–6000 m³/h for the process air and 0–2000 m³/h for the regeneration air. Fig. 1(b) presents a photographic view of the experimental system, and detailed information of the desiccant wheel and the dehumidification system is provided in Appendix A.

The purpose of the experiments was to evaluate the performance of the desiccant wheel dehumidification process to produce air with low dew point temperature. Therefore, the experimental tests were set up to investigate the influence of the process air and regeneration air parameters as well as the operating parameters. Table 2 presented a series of basic experimental conditions, and the full test conditions were listed in Appendix B. Two different temperature and humidity ratio combinations of inlet process air were examined in the study to test the dehumidification performance, representing low humidity dehumidification and normal humidity dehumidification conditions, respectively. The combination of 6 °C and 4 g/kg was the typical outlet condition of liquid dehumidification system applied in low humidity industries, representing low humidity dehumidification condition; and the combination of 13 °C and 9 g/kg was the typical outlet condition of a conventional cooling system, representing normal humidity process. On the regeneration side, a series of regeneration temperatures from 60 to 120 °C and humidity ratio from 4 to 24 g/kg was examined. The

preliminary experiment was conducted to evaluate the effect of different rotation speeds on the dehumidification performance, which was also mentioned in section 3.2. It was found that 20 r/h was near optimum for the experimental conditions, therefore, this rotation speed was subsequently fixed in the study.

2.2. Instrumentation and measurement methodology

Measurements were conducted to investigate the actual performance of the desiccant wheel dehumidification system. The information on instrumentation used in the test is provided in Table 3, and the detailed measurement methodology is also introduced in Appendix A. On both dehumidification and regeneration sides, the temperature and humidity meters were installed to monitor the air parameter at the inlet and the outlet of the desiccant wheel as well as the inlet of the air tunnel. The airflow rate was controlled by the damper and measured volumetrically using an anemometer.

The sensible heat and mass balance between the process air and the regeneration air have been verified in each experimental test, and the differences in variance are within ± 15%, as shown in Fig. 2. The deviation errors have been found within the acceptable limit and the experimental results are proved reliable for further analysis.

2.3. Performance indexes

To evaluate the system performance of the desiccant wheel, the following indexes were analyzed in the study.

(1) Relative dehumidification capacity.

The dehumidification capacity ($\Delta\omega_p$, g/kg) represents the performance of the dehumidification amount of the desiccant wheel, which can be defined as the humidity ratio difference between inlet process air and outlet process air:

$$\Delta\omega_p = \omega_{p,in} - \omega_{p,out}$$

where $\omega_{p,in}$ (g/kg) and $\omega_{p,out}$ (g/kg) are the humidity ratio of inlet process air and outlet process air, respectively.

The relative dehumidification capacity (RDC, dimensionless) can be defined as the dehumidification capacity of the desiccant wheel in relation to the humidity ratio of inlet process air:

$$RDC = \frac{\Delta\omega_p}{\omega_{p,in}}$$

It is worth noting that the ideal maximum dehumidification capacity is not 100% because the minimum humidity ratio of outlet process air is achieved when the equilibrium water content between process air and solid desiccant equals to that between inlet regeneration air and solid desiccant.

(2) Dehumidification coefficient of performance.

Thermal power is provided to the regeneration air in the system to reach the required regeneration temperature, and it can be obtained from the regeneration airflow and the temperature difference between the regeneration temperature and the ambient temperature as follows.

$$q_{in} = \rho_a c_{p,a} m_r (t_{r,in} - t_{r,amb})$$

Where q_{in} (kW) is the thermal consumption provided to the regeneration air, ρ_a (kg/m³) is the density of air, $c_{p,a}$ (kJ/(kg·K)) is the specific heat capacity of air, m_r (m³/s) is the flowrate of regeneration air, $t_{r,in}$ (K) is the regeneration temperature, and t_{amb} (K) is the ambient temperature, which is considered at 25 °C in the study for further discussion.

The dehumidification coefficient of performance (DCOP, dimensionless) can be defined as the dehumidification capacity of the desiccant wheel in relation to the required heat supplied to the regeneration air, which also represents the energy efficiency of the desiccant wheel:

$$DCOP = \frac{\rho_a m_r \cdot \Delta\omega_p}{1000 q_{in}}$$

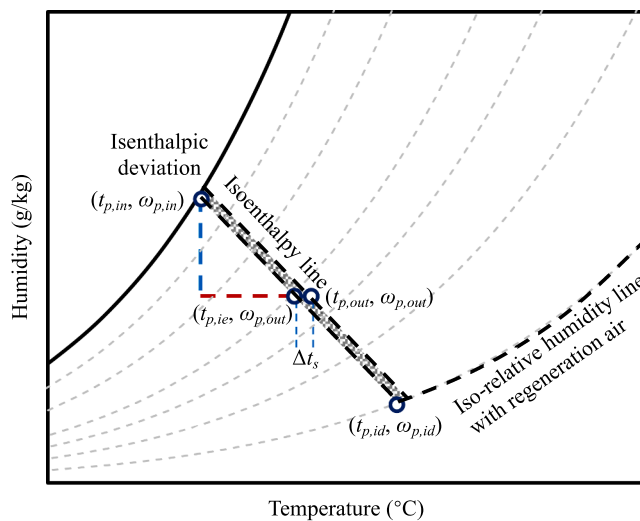


Fig. 3. Thermodynamic description of the isenthalpic deviation and surplus temperature rise on the psychrometric chart.

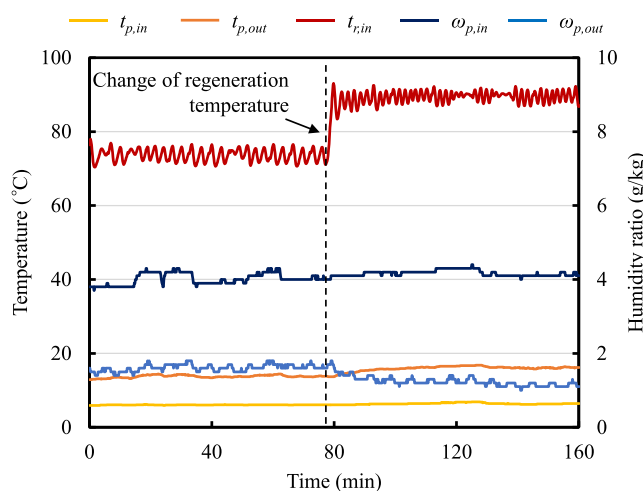


Fig. 4. Time dependence of the outlet air parameters varying with regeneration temperature ($\omega_{r,in} = 24$ g/kg).

where m_p (m^3/s) is the flow rate of regeneration air, and r (kJ/kg) is the latent heat of vaporization of moisture.

(3) Effectiveness parameter.

The ideal desiccant wheel dehumidification process is an isenthalpic process, however, due to the irreversible heat loss from the desiccant material and the framework, there is certain isenthalpic deviation during the actual dehumidification process, resulting in surplus temperature rise at the outlet state of process air. The description of the isenthalpic deviation and the surplus temperature rise is presented on the psychrometric chart as Fig. 3 shown.

The isenthalpic deviation (η_h , dimensionless) of the desiccant wheel can be defined as the relative deviation of enthalpy of the inlet and outlet process air:

$$\eta_h = \frac{h_{p,out} - h_{p,in}}{h_{p,in}}$$

where $h_{p,out}$ (kJ/kg) is the enthalpy of outlet process air, and $h_{p,in}$ (kJ/kg) is the enthalpy of inlet process air. Ideally, the desiccant wheel dehumidification process is the isenthalpic process and η_h of the desiccant wheel is equal to 0. However, the heat capacity of the desiccant substrate and the water content leads to incomplete heat and exchange between humid air and the solid desiccant, resulting in the isenthalpic

deviation and $\eta_h > 0$ for the actual desiccant wheel dehumidification process.

A brand effectiveness parameter, the surplus temperature rise (Δt_s , °C), is also introduced in the study, which is defined as the temperature difference between $t_{p,out}$ and $t_{p,ie}$ as follows:

$$\Delta t_s = t_{p,out} - t_{p,ie}$$

where $t_{p,out}$ (°C) is the temperature of outlet process air, and $t_{p,ie}$ (°C) is the temperature corresponding to the outlet process humidity ratio and inlet process air enthalpy.

The surplus temperature deviation (η_t , dimensionless) of the desiccant wheel can be defined as the ratio of Δt_s to the overall temperature rise of the process air:

$$\eta_t = \frac{\Delta t_s}{t_{p,out} - t_{p,in}}$$

Compared to the isenthalpic deviation, the surplus temperature rise is characterized by temperature, which is independent from the humidity ratio of the process air. It can effectively indicate the irreversible heat loss on the air temperature changes during the deep dehumidification process of desiccant wheel.

3. Experimental results

3.1. Inertia of the test system

The inertia of the test device was evaluated in the study to indicate the time required for the system to regain a steady state after a change of the operation parameters. Fig. 4 shows the time dependence of the outlet air parameters when changing the regeneration temperature. It was indicated that the time period required to regain a steady state after the parameter change was about 10 to 20 min. Therefore, the tests were carried out after the outlet air parameters reached stability and continuously measured for around 30 min.

3.2. Effect of rotation velocity

The effects on the outlet temperature and humidity ratio of process air are presented in Fig. 5 as the rotation speed varies from 10 r/h to 30/r/h. The regeneration side is operated at the constant regeneration temperature of 90 °C and the humidity ratio of 4 g/kg. As the rotation speed increases, the outlet temperature of process air also rises remarkably, while the outlet humidity of process air decreases firstly and increases subsequently, resulting in the dehumidification process gradually deviating from the isenthalpic process as the rotation speed increases. As shown in Fig. 6, the difference of isenthalpic deviation between different rotation speeds is more significant for low humidity dehumidification process than normal humidity dehumidification process. With the rotation speed increasing from 10 r/h to 30 r/h, the isenthalpic deviation for the normal humidity dehumidification process slightly increases from 4.8% to 11.6%. However, it varies rapidly from 9.9% to 26.7% for low humidity dehumidification process. It illustrates that the rotation speed has a more significant influence on the dehumidification performance process under low humidity condition than conventional condition since the latent heat treatment process has an increasing demand for the energy input with the deepening of dehumidification process, which will be further discussed in section 3.3 and section 4.1. The results indicate that 20 r/h was near optimum for both low humidity and normal humidity dehumidification conditions to achieve the lowest outlet humidity ratio of process air. Therefore, this rotation speed was subsequently fixed at 20 r/h in this study.

3.3. Comparison of normal and low humidity dehumidification

To illustrate the performance difference between normal and low

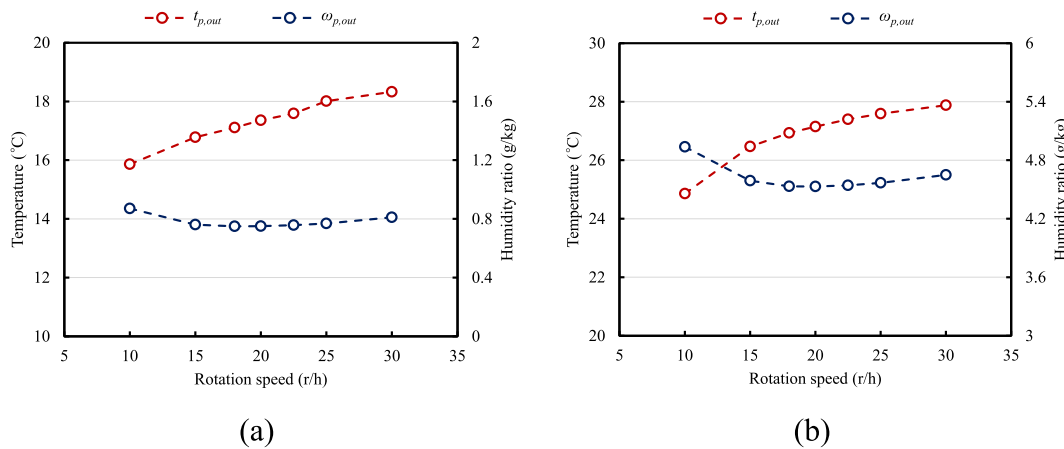


Fig. 5. Effects of rotation speed variance on outlet temperature and humidity of process air: (a) $t_{p,in} = 6^\circ\text{C}$, $\omega_{p,in} = 4 \text{ g/kg}$, and (b) $t_{p,in} = 13^\circ\text{C}$, $\omega_{p,in} = 9 \text{ g/kg}$.

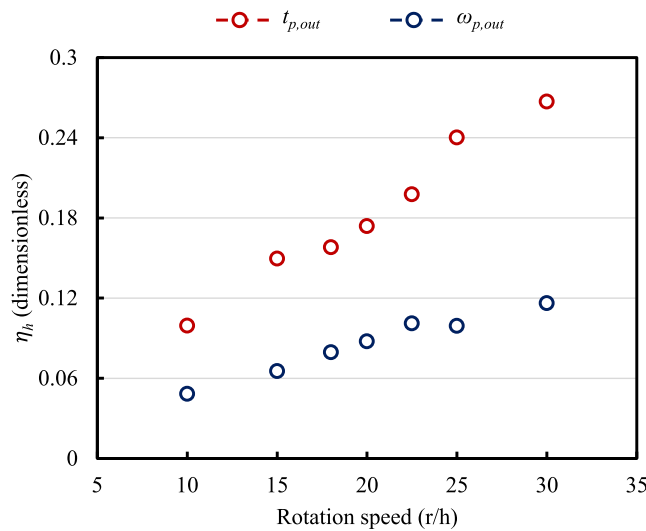


Fig. 6. Effects of rotation speed variance on the isenthalpic deviation of process air.

humidity dehumidification process, the outlet process air and regeneration air states at the optimum rotation speed are presented on the psychrometric chart, shown in Fig. 7. In addition, Fig. 8 shows the dehumidification and energy performance of the system as the regeneration temperature increases between normal and low humidity dehumidification process. The experimental results indicate that inlet temperature and humidity ratio have a significant impact on the dehumidification performance of the desiccant wheel. The inlet condition of 6°C and 4 g/kg appears to have lower outlet humidity ratio of process air regardless of the variation in regeneration temperature and humidity ratio compared to normal inlet conditions. When $\omega_{r,in} = 4 \text{ g/kg}$, the desiccant wheel can effectively remove the moisture of the process air from 4 g/kg to less than 1 g/kg under $t_{r,in} = 75 \sim 105^\circ\text{C}$, and within the range of experimental results, the dehumidification system can achieve the lowest outlet humidity ratio at around 0.60 g/kg when running under $t_{r,in} = 105^\circ\text{C}$. In addition, low inlet condition of process air shows higher RDC of the desiccant wheel compared to high inlet conditions, reaching from 77.4% to 85.2% at $\omega_{r,in} = 4 \text{ g/kg}$, but it shows smaller DCOP from 0.45 to 0.33 because of less amount of the total dehumidification capacity. This means that the reduction of inlet condition of process air can increase the adsorption thrust force on the dehumidification side which leads to the relative dehumidification performance to improve and reduces the outlet air humidity ratio. With the increase in

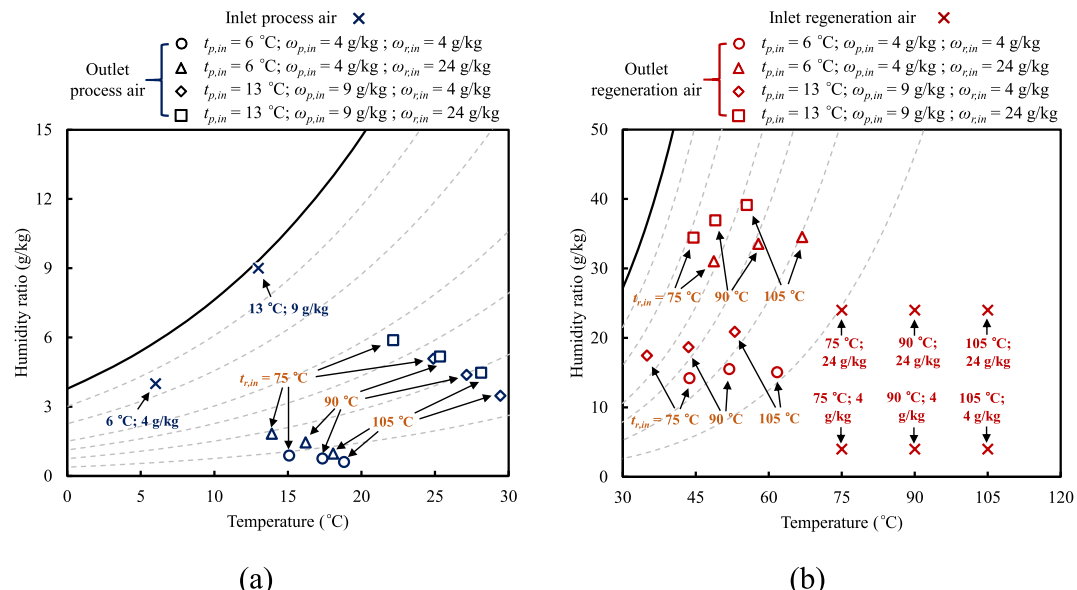


Fig. 7. The outlet process air and regeneration air states presented on the psychrometric chart: (a) Process air, and (b) Regeneration air.

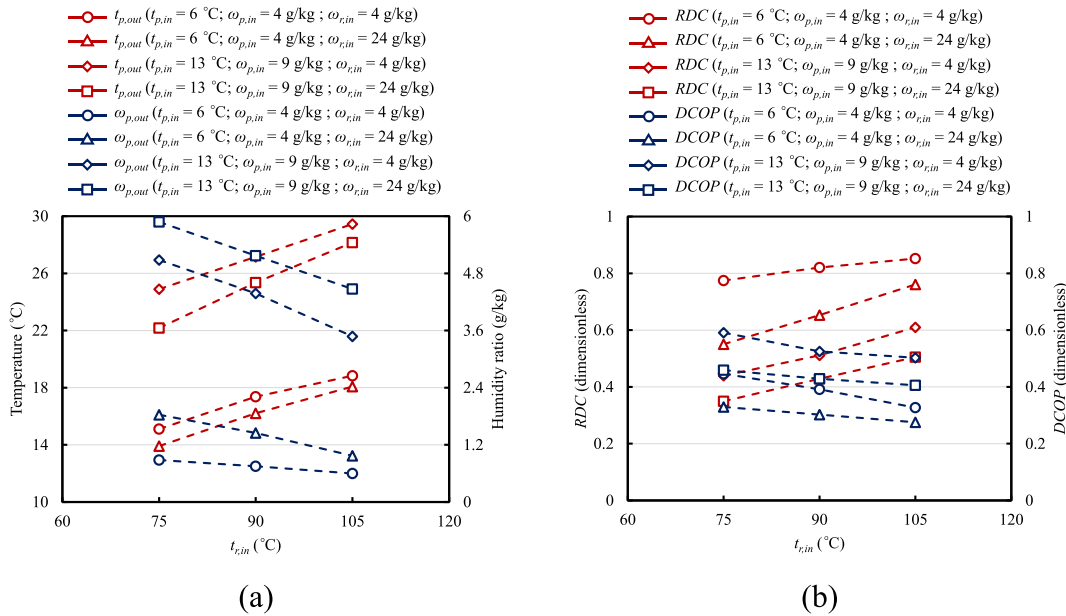


Fig. 8. Dehumidification and energy performances of the system: (a) Outlet temperature and humidity of process air, and (b) RDC and DCOP.

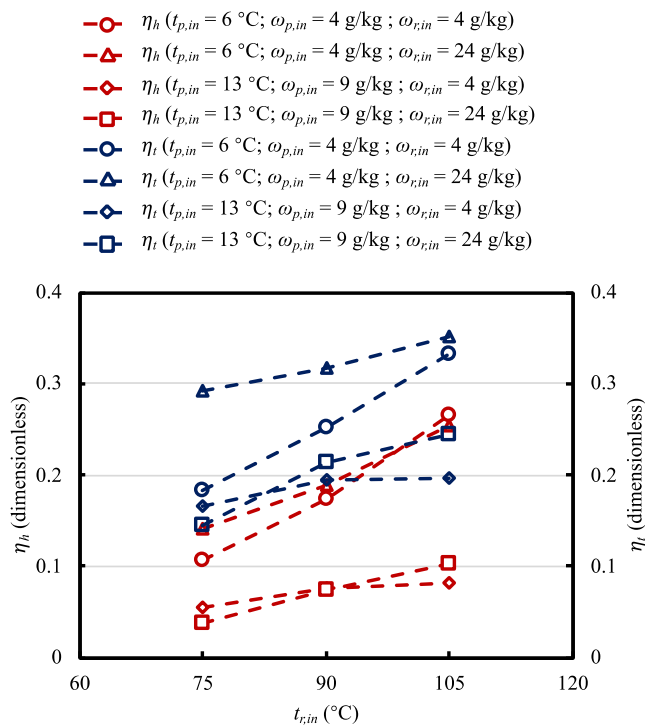


Fig. 9. Isenthalpic deviation and surplus temperature effectiveness of the system.

the regeneration temperature and decrease in the regeneration humidity ratio, the regeneration side has stronger adsorption thrust force, and the system can reach lower outlet humidity ratio as a result.

Fig. 9 indicates the isenthalpic deviation and the surplus temperature effectiveness of the system between normal and low inlet conditions of process air. The η_h in normal inlet conditions ranges from 5.5% to 10.2% when the regeneration parameters change, however, it is around 10.7% to 26.4% in low inlet conditions. The results indicate that low inlet conditions have much higher isenthalpic deviation than normal inlet conditions. Although the surplus temperature rise is caused by the isenthalpic deviation, the surplus temperature deviation of the

dehumidification process is more significant than the isenthalpic deviation. The trend of η_t is consistent with that of during the dehumidification process, ranging from 16.6% to 24.4% in normal inlet conditions and from 18.3% to 35.2% in low inlet conditions. Higher isenthalpic deviation also leads to significant surplus temperature rise, and the deep dehumidification process also shows significant larger surplus temperature deviation compared to normal dehumidification process. The surplus temperature rise can be up to 4.16 °C at $\omega_{r,in} = 24$ g/kg, accounting for 35.2% of the total temperature rise of process air, resulting in large amount of heat loss. This means that with the deepening of dehumidification process, a greater part of the input energy is transformed into sensible heat exchange between air and desiccant due to the heat capacity of desiccant substrate and water content, and less is transformed into adsorption thrust force for dehumidification demand. It can be speculated that with the input regeneration energy force further rising, the isenthalpic deviation in low inlet conditions of process air will also significantly increase, and it will be more difficult to reduce the outlet air humidity ratio to a deeper level. It can be also seen that there is a smaller isenthalpic deviation and surplus temperature deviation at $\omega_{r,in} = 4$ g/kg than 24 g/kg for low inlet process air parameters under low regeneration temperature, and the isenthalpic deviation is smaller at $\omega_{r,in} = 24$ g/kg for normal inlet process air parameters. However, it is observed to have an opposite tendency of isenthalpic deviation and surplus temperature deviation under high regeneration temperature. Since the enthalpy change of the desiccant wheel is very small, the results may get affected by the measuring error. The major reason that the isenthalpic deviation shows the opposite tendency under different inlet conditions is the temperature and humidity ratio difference between the regeneration side and the dehumidification side that influences the heat and mass exchange during the dehumidification process.

3.4. Effect of process air temperature and humidity ratio

The previous section has addressed the comparison of dehumidification performance between normal and low inlet process conditions. It reveals that process air condition is one of the major factors that determine the dehumidification depth of the desiccant wheel. Therefore, the influence of process air parameters on the dehumidification performance is discussed in this section. Multiple combinations of inlet temperature and humidity ratio are measured in the study, ranging from

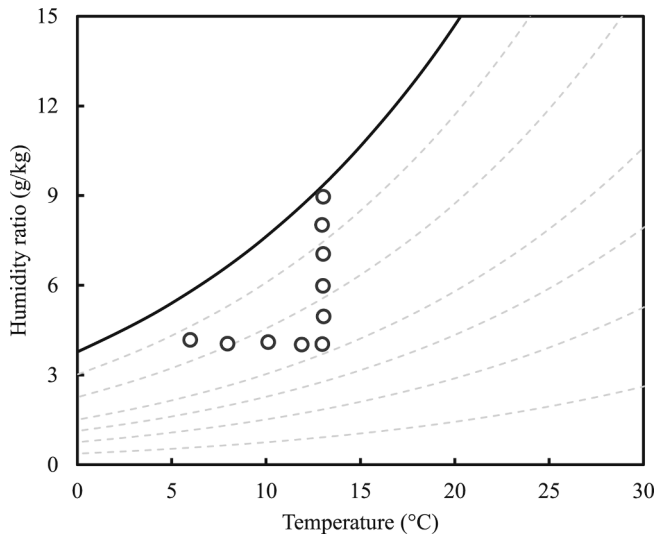


Fig. 10. The experimental inlet conditions of process air presented on the psychrometric chart.

6 °C to 13 °C in temperature and from 4 g/kg to 9 g/kg in humidity ratio, and the regeneration air is controlled at 90 °C and 4 g/kg. The experimental inlet conditions of process air can be seen from the psychrometric chart in Fig. 10. Fig. 11 shows the dehumidification and energy

performance of the system when changing the inlet parameters of process air. It can be seen that as the inlet temperature decreases, lower outlet humidity ratio can be reached, and higher RDC and DCOP can be achieved. This is because the decrease in process air temperature expands the difference of equilibrium content between process air and solid desiccant, which improves the ability to remove moisture from the process air. The inlet humidity ratio has a stronger effect on the outlet humidity ratio than inlet temperature. When the inlet humidity ratio varies from 4 g/kg to 9/kg at $t_{p,in} = 13$ °C, the outlet air humidity ratio also increases from 1.09 g/kg to 4.38 g/kg, and RDC decreases from 73.0% to 51.1%. With the increase of inlet humidity ratio, more moisture is removed during the dehumidification process so that DCOP of the system is improved from 0.33 to 0.52.

3.5. Effect of regeneration air temperature and humidity ratio

Previous discussion in section 3.3 has indicated that the outlet temperature of process air increases and the humidity ratio of process air decreases under higher regeneration temperature. The overall RDC increases and achieves over 80% when regeneration humidity is relatively low. Apart from the basic conditions, experiments are carried out to illustrate the effect of regeneration parameters on dehumidification and energy efficiency of the desiccant wheel. For low process air parameters, Fig. 12 summarizes the optimal results with regeneration temperature from 75 °C to 105 °C and regeneration humidity ratio from 4 g/kg to 24 g/kg. As expected, the desiccant wheel achieves better dehumidification performance under high regeneration temperature. On the other hand,

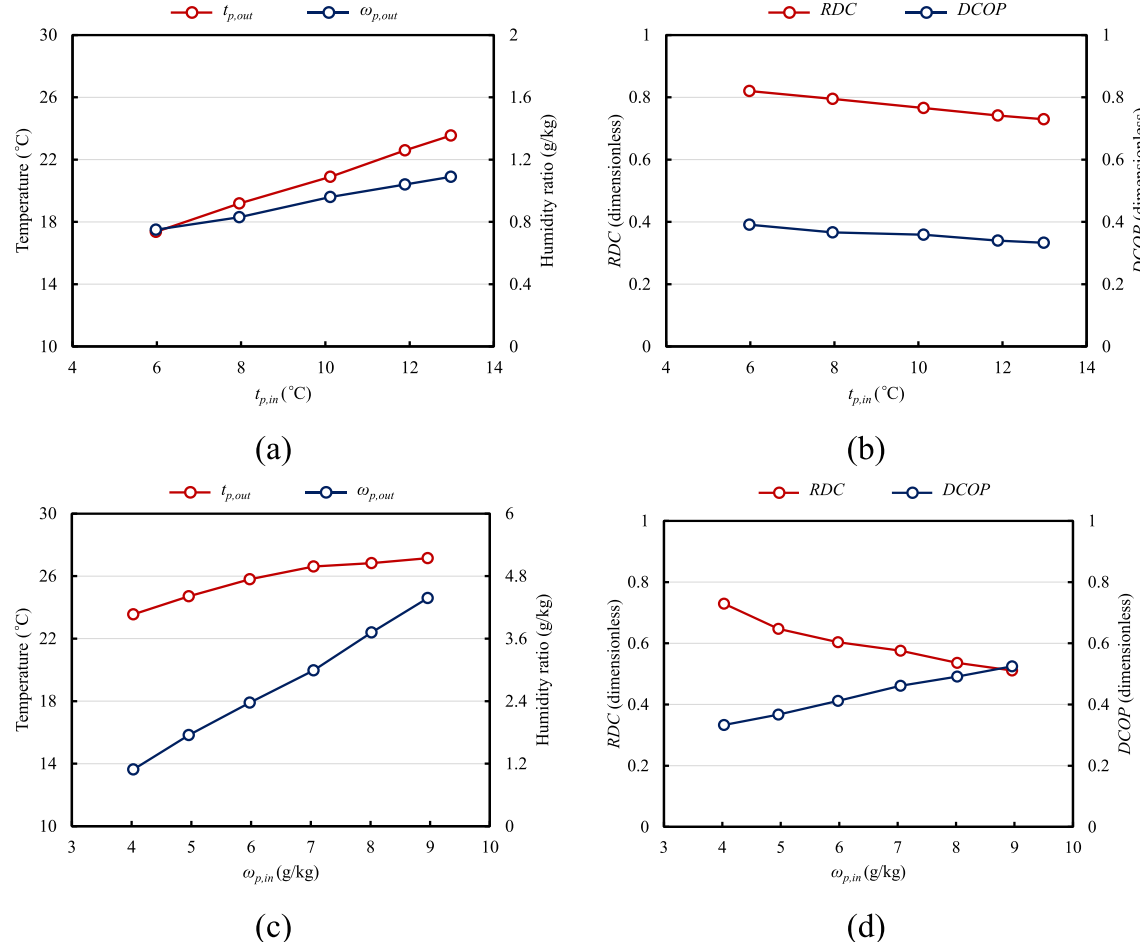


Fig. 11. Dehumidification and energy performances of the system: (a) Outlet temperature and humidity of process air ($t_{p,in} = 6 \sim 13$ °C, $\omega_{p,in} = 4$ g/kg), (b) RDC and DCOP ($t_{p,in} = 6 \sim 13$ °C, $\omega_{p,in} = 4$ g/kg), (c) Outlet temperature and humidity of process air ($t_{p,in} = 13$ °C, $\omega_{p,in} = 4 \sim 9$ g/kg), and (d) RDC and DCOP ($t_{p,in} = 13$ °C, $\omega_{p,in} = 4 \sim 9$ g/kg).

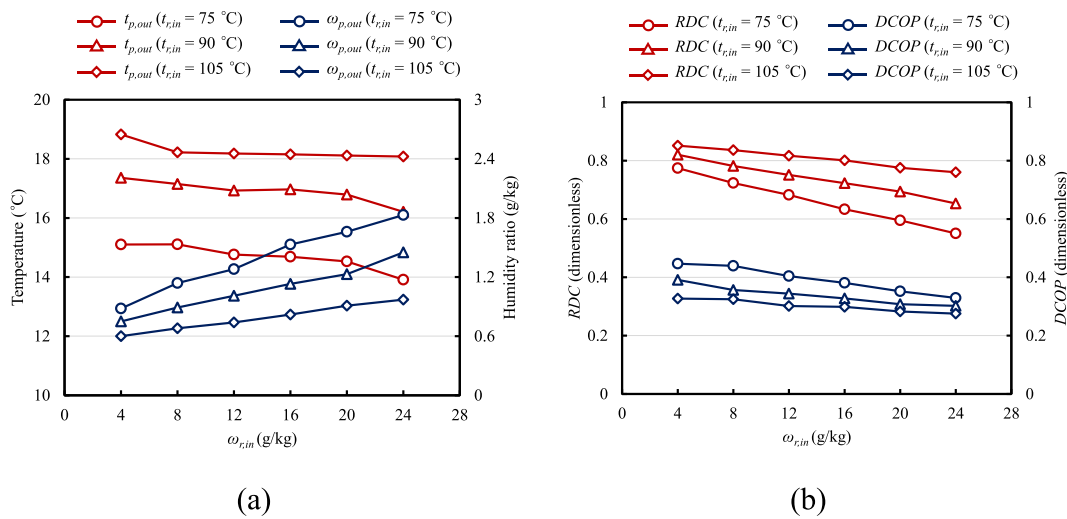


Fig. 12. Dehumidification and energy performances of the system ($t_{p,in} = 6$ °C, $\omega_{p,in} = 4$ g/kg): (a) Outlet temperature and humidity of process air, and (b) RDC and DCOP.

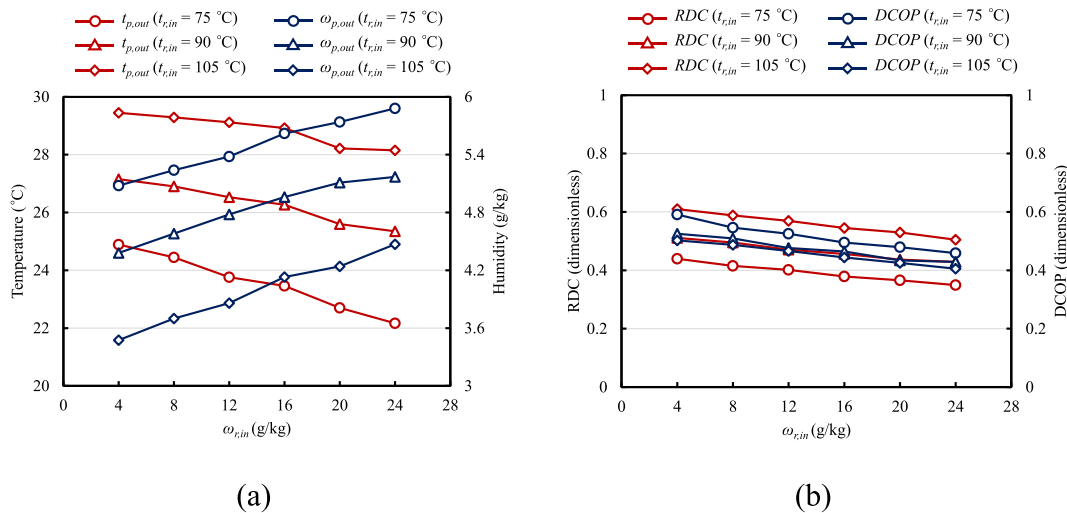


Fig. 13. Dehumidification and energy performances of the system ($t_{p,in} = 13$ °C, $\omega_{p,in} = 9$ g/kg): (a) Outlet temperature and humidity of process air, and (b) RDC and DCOP.

although RDC improves under the condition of higher regeneration temperature, the system appears to consume larger amount of thermal energy. Therefore, the increase in regeneration temperature results in lower DCOP for the system.

The results also indicate that the outlet temperature of process air has a slight decrease but the outlet humidity ratio increases with the rise of regeneration humidity. Both RDC and DCOP can enhance under lower regeneration humidity. The outlet humidity ratio of process air slightly drops from 0.88 g/kg to 0.60 g/kg when regeneration temperature rises from 75 °C to 105 °C under regeneration humidity ratio of 4 g/kg. However, under relatively high regeneration humidity, the air humidity of process air is more sensitive to the variation of regeneration temperature. When the regeneration humidity ratio rises to 24 g/kg, the outlet humidity ratio of process air can be reduced to 0.97 g/kg under regeneration temperature of 105 °C, and 47% of the process air humidity can be further reduced when regeneration temperature rises from 75 °C to 105 °C.

Within the experimental range of regeneration humidity, there is a slight change of RDC for relatively high regeneration temperature conditions. However, regeneration humidity shows a strong effect on the variation of RDC under low regeneration temperature. Under the

regeneration temperature of 105 °C, RDC of the system only decreases by 9.1% when regeneration humidity ratio ranges from 4 g/kg to 24 g/kg, however, it will rapidly decrease from 77.4% to only 55.0% under the regeneration temperature of 75 °C. Similarly, DCOP also shows a slight decrease from 0.45 to 0.33 at high regeneration temperature and a relatively large gap at low regeneration temperature.

For normal process air parameters, Fig. 13 also summarizes the results with the change of regeneration conditions. The results show high consistency with low process air parameters. The overall outlet process air humidity ratio is relatively higher, and RDC is not as efficient as low humidity conditions of process air. DCOP is higher for normal humidity dehumidification because of the large moisture removal amount. In addition, for normal process air parameters, the dehumidification capacity of the desiccant wheel does not reach the maximum dehumidification capacity within the experimental range of regeneration temperature and humidity, so there is no significant change in the gradient variation of outlet process air temperature and humidity.

3.6. Effect of airflow rate

Fig. 14 shows the outlet temperature and humidity ratio of process

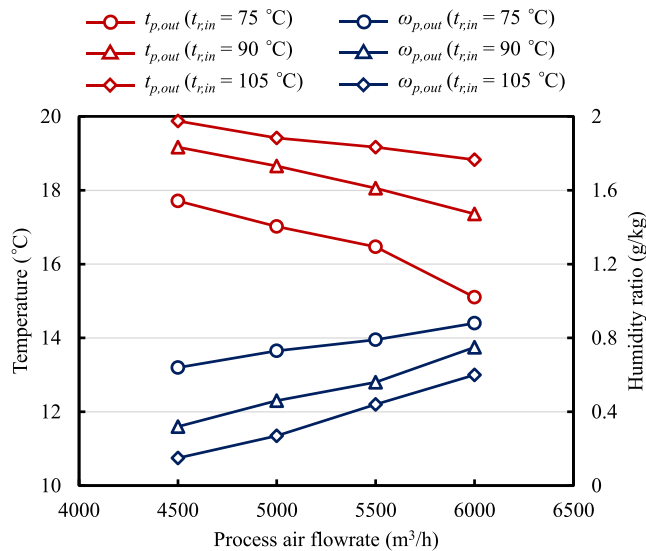


Fig. 14. Dehumidification performance of the system varying with air flowrate.

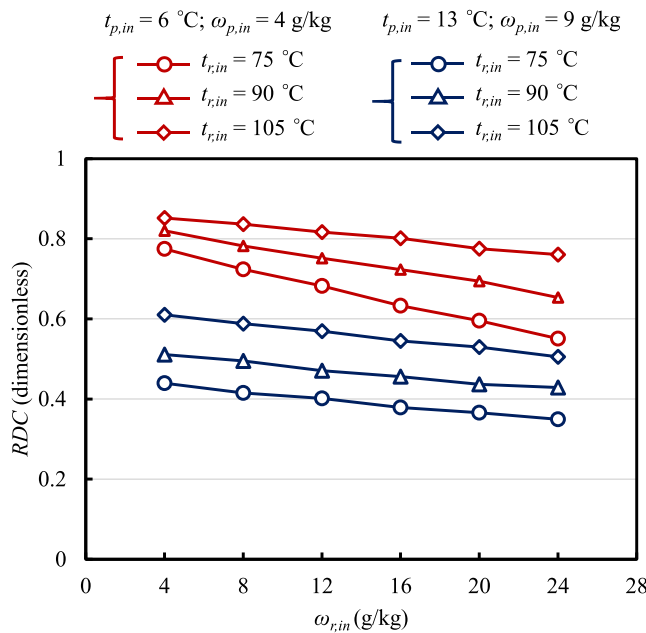


Fig. 15. RDC of the system under different experimental conditions.

air as airflow rate changes from 4500 m³/h to 6000 m³/h. The outlet humidity ratio of process air decreases with a decreasing airflow rate, and it is more significant under high regeneration temperature. This is because the decline of air velocity helps to enhance the latent heat and mass transfer efficiency between air stream and solid desiccant, which improves the dehumidification capacity as a result.

4. Discussion

4.1. Sensitivity to process and regeneration parameters

As mentioned above, the desiccant wheel dehumidification system can show relatively higher RDC when the process side is under low temperature and low humidity. In addition, the RDC of the desiccant wheel also increases with the rising of regeneration temperature and the reduction of regeneration humidity. In this section, the sensitivity of parameter changes in the process side and regeneration side to the

maximum dehumidification depth and RDC will be further discussed.

Fig. 15 concludes the RDC of the system under different process and regeneration conditions. It can be seen from the experimental results that under the inlet process air of 6 °C and 4 g/kg, the effect of the regeneration temperature on the dehumidification performance weakens as the regeneration humidity becomes lower. For example, when the regeneration air is 4 g/kg, the RDC of the system reaches 77.4% under the regeneration temperature of 75 °C, but it only increases by about 7.7% with the regeneration air further increasing to 105 °C. When the regeneration humidity is relatively high, however, the improvement of RDC shows an evident increase with the regeneration temperature rising from 75 °C to 105 °C. The RDC can increase by about 13.4% under the regeneration humidity ratio of 12 g/kg and about 21.0% under 24 g/kg. Therefore, it can be concluded that the change of regeneration temperature shows higher sensitivity to the improvement of the dehumidification performance of the desiccant wheel under higher regeneration humidity. In particular, the RDC of the desiccant wheel is nearly independent of the regeneration temperature under the condition of very low regeneration humidity. Under the inlet process air of 6 °C and 4 g/kg, however, the RDC of the desiccant wheel has similar enhancement with the increase of regeneration temperature regardless of the regeneration humidity. The increase of RDC as the regeneration temperature rises for different regeneration humidity is between 15.5% and 17.3%, and the difference is presumably mainly caused by measurement biases. Similarly, the sensitivity of dehumidification performance to the change of regeneration humidity is reduced when the desiccant wheel is operated at high regeneration temperature, and the RDC of the system exhibits high independence of the variation of regeneration humidity. On the other hand, the RDC quickly decreases with the increase of regeneration humidity under low regeneration temperature.

For the dehumidification side, lower process air temperature and humidity help to improve the dehumidification capacity and obtain lower outlet process air humidity. If the inlet process temperature and humidity are relatively high, the RDC can only reach about 60% even when the system is operated at very high regeneration temperature and very low regeneration humidity, and it has a higher sensitivity to the regeneration parameters. In conclusion, when there are several parameters such as process air temperature and humidity, regeneration temperature and humidity, and other parameters leading the desiccant wheel to operate with relatively high-efficient inlet conditions, the desiccant wheel dehumidification system can work stably while maintaining high dehumidification performance and be less sensitive to the variances of other parameters.

4.2. Effectiveness parameter analysis

Fig. 16(a) presents the relationship between the effectiveness parameters η_h and η_t under different inlet process and regeneration air conditions. It can be indicated that η_h and η_t of the dehumidification process is generally positively correlated. Influenced by the inlet parameters of both process air and regeneration air, larger isenthalpic deviation also leads to larger surplus temperature deviation. For a certain dehumidification inlet process air state, η_h and η_t are roughly maintaining within a parallelogram range with the variation of regeneration air temperature and humidity ratio, which is also indicated in Fig. 16(a). It is concluded that the deep dehumidification process has significant higher thermodynamic deviation compared with normal dehumidification process caused by irreversible heat loss. With the regeneration air temperature ranging from 75 °C to 105 °C and the regeneration air humidity ratio ranging from 4 g/kg to 24 g/kg under the inlet process air of 6 °C and 4 g/kg, the η_h of the desiccant wheel dehumidification process varies between 8.9% and 25.4%, and the η_t varies between 16.1% and 34.9%. Meanwhile, η_h and η_t only change from 3.7% to 10.2% and from 11.8% to 22.9% under the inlet process air of 13 °C and 9 g/kg, respectively. With the rise of regeneration

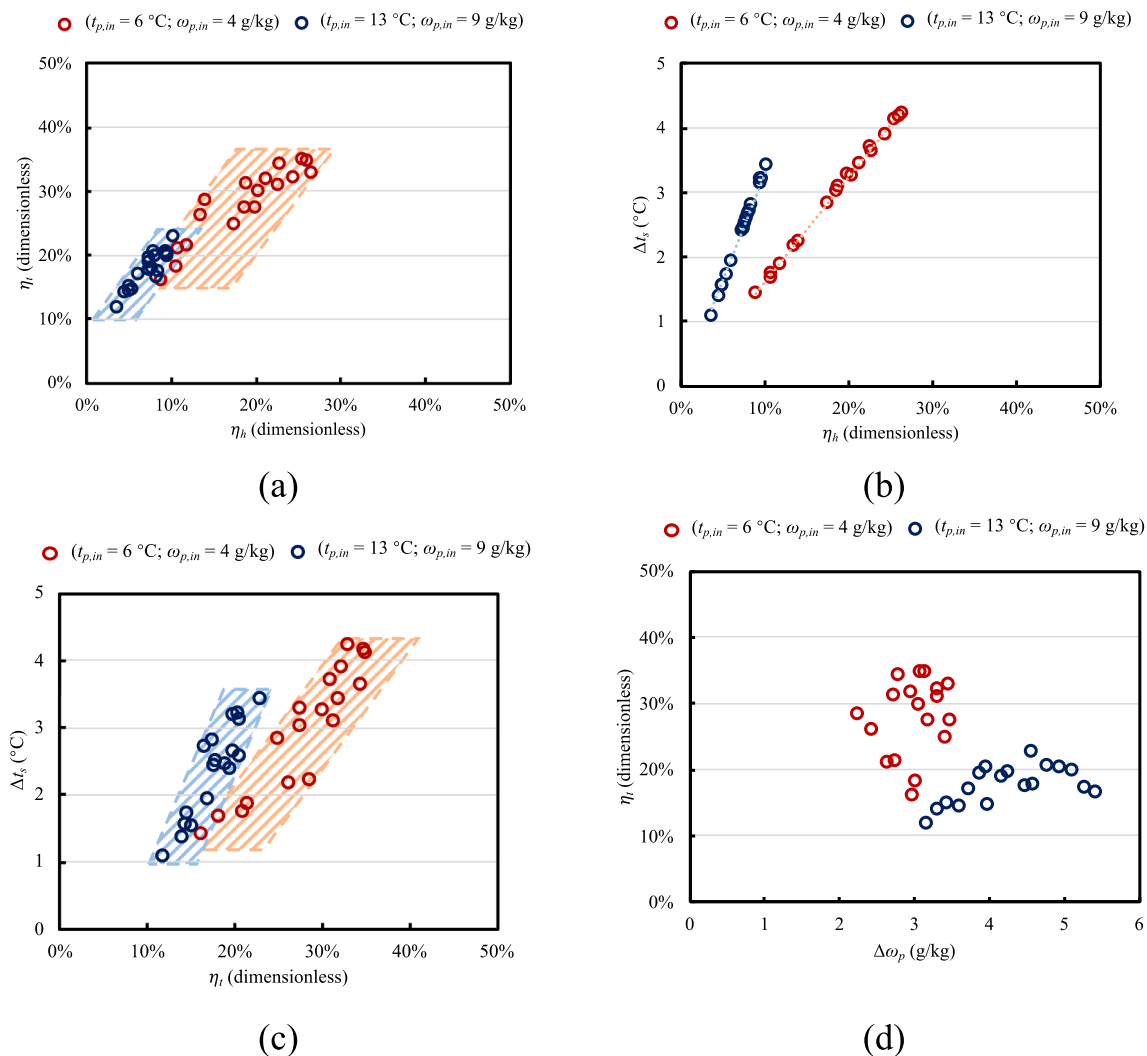


Fig. 16. Thermodynamic effectiveness analysis of the desiccant wheel.

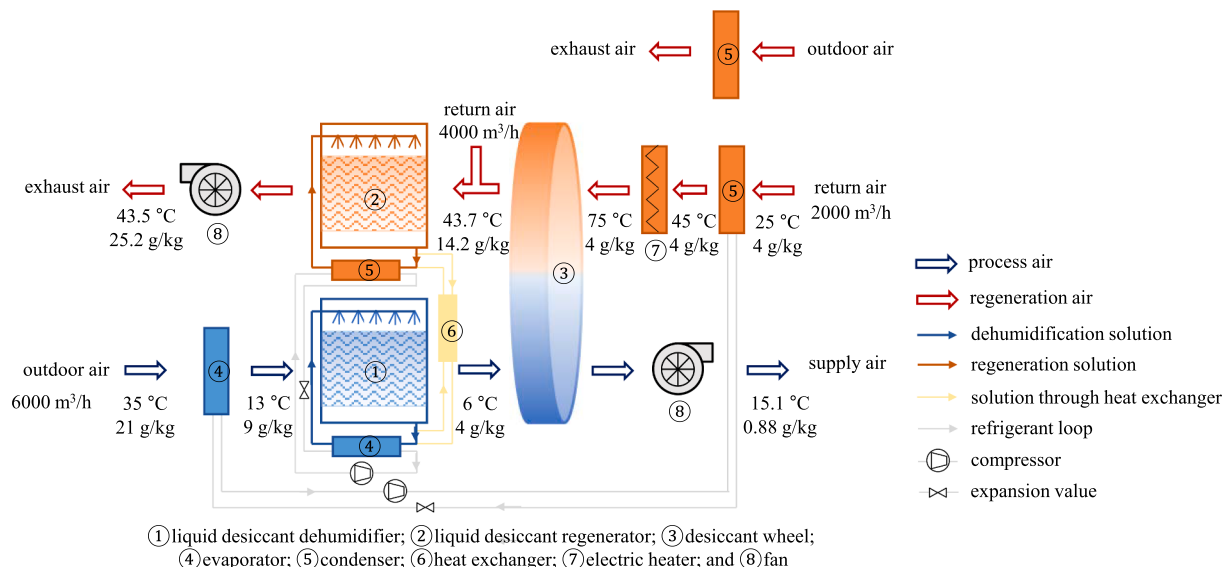


Fig. 17. Configuration and designed parameters of the proposed deep dehumidification system integrated with the desiccant wheel.

Table 4

Energy performance of the designed deep dehumidification system.

Dehumidification capacity (g/s)	Heat pump consumption for refrigeration cooling system (kW)	Heat pump consumption for liquid desiccant system (kW)	Electric Heating (kW)	COP_e (dimensionless)
6.04	23.8	10.2	20.0	1.86

Table A1

Detailed information of the desiccant wheel and the dehumidification system.

Desiccant wheel:	
Diameter (m)	0.8
Thickness (m)	0.2
Rotation speed (r/h)	20
ρ_{ad} (kg/m ³)	1129
$c_{p,ad}$ [J/(kg·K)]	920
χ (dimensionless)	0.7
Porosity (dimensionless)	0.7
W_{max} (dimensionless)	0.39
Air ducts:	
Process air ducts (m ² m)	0.5*0.25
Regeneration air ducts (m ² m)	0.32*0.25

temperature, both η_h and η_t significantly increase, which is because greater heat loss occurs in the heating process of the desiccant materials due to the increasing temperature difference. η_h and η_t also increase at lower regeneration temperature with the increase of regeneration humidity ratio, but there is only a slight change at higher regeneration temperature, and the variation of the thermodynamic deviations to the change of regeneration humidity ratio is less evident under normal dehumidification process. Fig. 16(b) shows the relationship between Δt_s and η_h . Δt_s and η_h are approximately linear under the same inlet process air states. It is obviously known that the slope of the Δt_s - η_h line is approximately $h_{p,in}/c_p$ based on the definition of the effectiveness parameters. Therefore, the Δt_s of deep dehumidification process is lower than normal dehumidification process under the same isenthalpic deviation, and on the contrary, larger isenthalpic deviation is observed in deep dehumidification process with the same degrees of surplus temperature rise. The relationship between Δt_s and η_t is also presented in Fig. 16(c), and they can also be expressed by a parallelogram framework

as the regeneration air temperature and humidity ratio change. The surplus temperature rise of deep dehumidification process is relatively higher than normal dehumidification, as well as η_t . Fig. 16(d) further presents the relationship between η_t and the dehumidification capacity $\Delta\omega_p$. Even though the deep dehumidification process generally shows higher η_t than normal dehumidification process, the association between η_t and $\Delta\omega_p$ is not remarkable. The main reason is that the dehumidification capacity depends on the regeneration air temperature and humidity ratio, and the surplus temperature rise has highly positive relevance to the regeneration air temperature but is not closely related to the regeneration air humidity ratio.

4.3. Application potential in deep dehumidification fields

It can be demonstrated that lowering the inlet temperature and humidity of process air can improve the dehumidification performance of the desiccant wheel, and lower outlet process air humidity can be obtained under relatively low regeneration temperature. At the inlet process condition of 6 °C and 4 g/kg, the dehumidification system can achieve the depth of 1 g/kg under the regeneration air temperature below 75 °C. Therefore, the desiccant wheel can be an alternative as the final stage of the cascading deep dehumidification system to dehumidify the hot and humid air to the depth of less than 1 g/kg. It can be integrated with the liquid desiccant dehumidification system to dehumidify the outdoor air to the required low humidity and realize the deep dehumidification process in the actual deep dehumidification fields, and one configuration of the integrated system is shown in Fig. 17. Similar configurations of the integrated dehumidification system are also proposed and investigated in other studies carried out by the authors. There have been sufficient studies that investigated the adoption of the liquid desiccant system to obtain the air humidity ratio of around 4 g/kg [30,33–35]. Using return air at 4 g/kg as the regeneration air, it can effectively treat the hot and humid outdoor air from 35 °C, 21 g/kg to

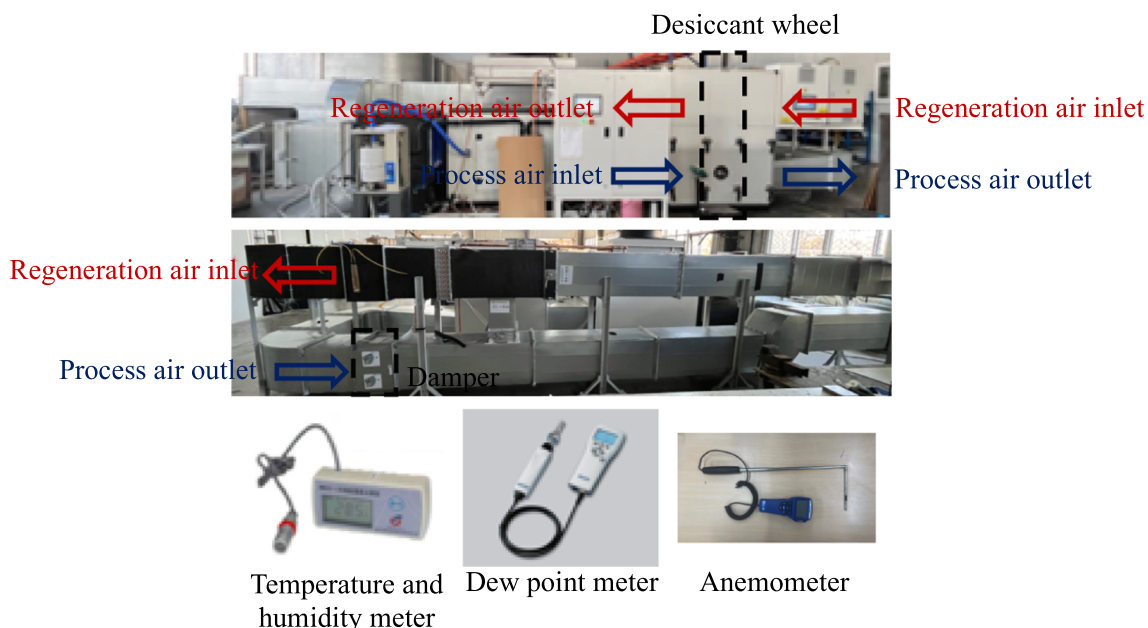
**Fig. A1.** Detailed instrumentation and measurement methodology.

Table B1

Summary of full experimental results.

Number	Designed parameters							Experimental results											
	$t_{p,in}$ (°C)	$\omega_{p,in}$ (g/ kg)	m_p ($\text{m}^3/$ h)	$t_{r,in}$ (°C)	$\omega_{r,in}$ (g/ kg)	m_r ($\text{m}^3/$ h)	Rotation velocity (r/h)	$t_{p,in}$ (°C)	$\omega_{p,in}$ (g/ kg)	$t_{r,in}$ (°C)	$\omega_{r,in}$ (g/ kg)	$t_{p,out}$ (°C)	$\omega_{p,out}$ (g/ kg)	$t_{r,out}$ (°C)	$\omega_{r,out}$ (g/ kg)	RDC	DCOP	η_h	η_t
<i>Basic conditions</i>																			
1	6	4	6000	75	4	2000	20	5.90	3.90	75.10	4.00	15.10	0.88	43.70	14.20	77.4%	0.45	10.7%	18.3%
2	6	4	6000	90	4	2000	20	5.98	4.17	89.80	4.06	17.36	0.75	51.88	15.50	82.0%	0.39	17.4%	25.1%
3	6	4	6000	105	4	2000	20	5.97	4.05	103.22	3.87	18.83	0.60	61.70	15.05	85.2%	0.33	26.4%	33.1%
4	6	4	6000	75	24	2000	20	6.06	4.07	73.61	23.77	13.91	1.83	48.70	31.04	55.0%	0.33	14.0%	29.2%
5	6	4	6000	90	24	2000	20	6.27	4.18	89.58	24.23	16.21	1.45	57.85	33.54	65.3%	0.30	18.8%	31.7%
6	6	4	6000	105	24	2000	20	6.25	4.05	105.00	24.10	18.08	0.97	66.85	34.54	76.1%	0.28	25.4%	35.2%
7	13	9	6000	75	4	2000	20	13.05	9.06	74.90	4.01	24.89	5.08	34.94	17.47	43.9%	0.59	5.5%	16.6%
8	13	9	6000	90	4	2000	20	13.03	8.96	89.62	4.12	27.15	4.38	43.47	18.68	51.1%	0.52	7.7%	19.4%
9	13	9	6000	105	4	2000	20	13.00	8.91	105.10	4.12	29.45	3.48	53.01	20.88	61.0%	0.50	8.2%	19.6%
10	13	9	6000	75	24	2000	20	13.02	9.04	74.23	23.99	22.17	5.88	44.51	34.44	35.0%	0.46	3.7%	14.5%
11	13	9	6000	90	24	2000	20	13.09	9.05	89.74	23.88	25.35	5.17	49.01	36.93	42.9%	0.43	7.4%	21.5%
12	13	9	6000	105	24	2000	20	13.17	9.03	105.50	23.51	28.15	4.47	55.46	39.13	50.5%	0.41	10.2%	24.4%
<i>Changing rotation velocity</i>																			
13	6	4	6000	90	4	2000	10	6.05	4.15	90.60	4.01	15.86	0.87	57.29	14.99	79.0%	0.37	9.9%	16.7%
14	6	4	6000	90	4	2000	15	6.02	4.1	90.40	4.02	16.78	0.76	53.92	15.45	81.4%	0.38	15.0%	22.7%
15	6	4	6000	90	4	2000	18	6.11	4.12	90.20	3.98	17.11	0.75	52.68	15.50	81.8%	0.38	15.8%	23.6%
16	6	4	6000	90	4	2000	20	5.98	4.17	89.80	4.06	17.36	0.75	51.88	15.5	82.0%	0.39	17.4%	25.1%
17	6	4	6000	90	4	2000	22.5	6.06	4.09	89.50	4.06	17.59	0.76	50.69	15.48	81.5%	0.38	19.8%	27.4%
18	6	4	6000	90	4	2000	25	6.04	4.02	90.20	4.00	18.01	0.77	50.17	15.14	80.9%	0.37	24.0%	32.3%
19	6	4	6000	90	4	2000	30	5.96	4.05	90.50	3.95	18.33	0.81	48.44	14.84	80.2%	0.37	26.7%	36.1%
20	13	9	6000	90	4	2000	10	12.87	9.07	89.58	4.05	24.86	4.94	51.84	16.67	45.6%	0.47	4.8%	14.5%
21	13	9	6000	90	4	2000	15	13.12	9.02	89.75	4.11	26.47	4.59	46.29	18.09	49.1%	0.51	6.5%	16.6%
22	13	9	6000	90	4	2000	18	13.05	8.98	90.12	4.16	26.93	4.53	44.40	18.38	49.5%	0.51	7.9%	20.4%
23	13	9	6000	90	4	2000	20	13.03	8.96	89.62	4.12	27.15	4.53	43.47	18.48	49.4%	0.51	8.8%	22.1%
24	13	9	6000	90	4	2000	22.5	13.03	8.89	90.17	4.05	27.40	4.54	42.64	18.54	48.9%	0.49	10.1%	24.8%
25	13	9	6000	90	4	2000	25	12.97	9.03	89.74	4.11	27.59	4.57	41.85	18.54	49.4%	0.51	9.9%	24.2%
26	13	9	6000	90	4	2000	30	12.98	8.99	89.88	4.02	27.88	4.65	40.77	18.46	48.3%	0.50	11.6%	27.7%
<i>Changing process air parameters</i>																			
27	6	4	6000	90	4	2000	20	5.98	4.17	89.8	4.06	17.36	0.75	51.88	15.5	82.0%	0.39	17.4%	25.1%
28	8	4	6000	90	4	2000	20	7.96	4.05	90.12	4.02	19.18	0.83	52.33	14.86	79.5%	0.37	17.6%	28.5%
29	10	4	6000	90	4	2000	20	10.12	4.10	89.78	4.03	20.89	0.96	53.21	14.50	76.6%	0.36	14.3%	27.2%
30	12	4	6000	90	4	2000	20	11.89	4.02	89.96	3.98	22.59	1.04	53.92	14.10	74.1%	0.34	14.8%	30.4%
31	13	4	6000	90	4	2000	20	12.98	4.03	90.35	4.03	23.55	1.09	54.30	13.93	73.0%	0.33	13.9%	30.5%
32	13	5	6000	90	4	2000	20	13.05	4.96	89.77	4.05	24.71	1.75	51.13	14.35	64.7%	0.37	14.3%	31.2%
33	13	6	6000	90	4	2000	20	13.02	5.98	89.89	4.12	25.80	2.37	48.60	15.32	60.4%	0.41	13.4%	30.5%
34	13	7	6000	90	4	2000	20	13.03	7.05	90.22	4.05	26.62	2.99	46.59	16.76	57.6%	0.46	11.3%	31.3%
35	13	8	6000	90	4	2000	20	12.97	8.02	89.86	4.03	26.83	3.72	43.91	17.88	53.6%	0.49	9.5%	29.6%
36	13	9	6000	90	4	2000	20	13.03	8.96	89.62	4.12	27.15	4.38	43.47	18.68	51.1%	0.52	7.7%	25.6%
<i>Changing regeneration air parameters</i>																			
37	6	4	6000	75	4	2000	20	5.90	3.90	75.10	4.00	15.10	0.88	43.70	14.20	77.4%	0.45	10.7%	18.3%
38	6	4	6000	90	4	2000	20	5.98	4.17	89.80	4.06	17.36	0.75	51.88	15.50	82.0%	0.39	17.4%	24.8%
39	6	4	6000	105	4	2000	20	5.97	4.05	103.22	3.87	18.83	0.60	61.70	15.05	85.2%	0.33	26.4%	32.9%
40	6	4	6000	75	8	2000	20	6.22	4.12	74.90	7.95	15.11	1.14	44.56	18.20	72.3%	0.44	8.9%	16.1%
41	6	4	6000	90	8	2000	20	6.15	4.08	90.80	8.02	17.15	0.89	53.44	18.91	78.2%	0.36	18.6%	27.5%
42	6	4	6000	105	8	2000	20	6.26	4.15	103.55	8.07	18.22	0.68	63.55	19.32	83.6%	0.32	19.9%	27.4%
43	6	4	6000	75	12	2000	20	6.00	4.03	74.65	12.04	14.76	1.28	45.72	21.22	68.2%	0.40	11.9%	21.4%
44	6	4	6000	90	12	2000	20	6.04	4.06	89.68	12.11	16.93	1.01	53.75	22.45	75.1%	0.34	20.3%	29.9%
45	6	4	6000	105	12	2000	20	6.02	4.04	104.95	12.02	18.18	0.74	64.28	22.98	81.7%	0.30	24.4%	32.1%
46	6	4	6000	75	16	2000	20	6.32	4.17	75.22	16.25	14.69	1.53	47.75	24.83	63.3%	0.38	10.7%	21.0%

(continued on next page)

Table B1 (continued)

Number	Designed parameters							Experimental results												
	$t_{p,in}$ (°C)	$\omega_{p,in}$ (g/ kg)	m_p ($\text{m}^3/$ h)	$t_{r,in}$ (°C)	$\omega_{r,in}$ (g/ kg)	m_r ($\text{m}^3/$ h)	Rotation velocity (r/h)	$t_{p,in}$ (°C)	$\omega_{p,in}$ (g/ kg)	$t_{r,in}$ (°C)	$\omega_{r,in}$ (g/ kg)	$t_{p,out}$ (°C)	$\omega_{p,out}$ (g/ kg)	$t_{r,out}$ (°C)	$\omega_{r,out}$ (g/ kg)	RDC	DCOP	η_h	η_t	
14	47	6	4	6000	90	16	2000	20	6.15	4.08	90.26	15.98	16.97	1.13	55.75	25.87	72.3%	0.33	21.2%	31.8%
	48	6	4	6000	105	16	2000	20	6.19	4.12	105.12	16.07	18.15	0.82	65.10	26.94	80.1%	0.30	22.6%	31.0%
	49	6	4	6000	75	20	2000	20	6.25	4.10	74.89	20.11	14.53	1.66	48.94	27.72	59.5%	0.35	13.4%	26.1%
	50	6	4	6000	90	20	2000	20	6.16	4.02	90.23	19.88	16.79	1.23	55.60	29.35	69.4%	0.31	22.7%	34.3%
	51	6	4	6000	105	20	2000	20	6.08	4.05	104.86	20.23	18.11	0.91	66.12	30.59	77.5%	0.28	26.0%	34.7%
	52	6	4	6000	75	24	2000	20	6.06	4.07	73.61	23.77	13.91	1.83	48.70	31.04	55.0%	0.33	14.0%	28.5%
	53	6	4	6000	90	24	2000	20	6.27	4.18	89.58	24.23	16.21	1.45	57.85	33.54	65.3%	0.30	18.8%	31.2%
	54	6	4	6000	105	24	2000	20	6.25	4.05	105.00	24.10	18.08	0.97	66.85	34.54	76.1%	0.28	25.4%	34.9%
	55	13	9	6000	75	4	2000	20	13.05	9.06	74.90	4.01	24.89	5.08	34.94	17.47	43.9%	0.59	5.5%	14.6%
	56	13	9	6000	90	4	2000	20	13.03	8.96	89.62	4.12	27.15	4.38	43.47	18.68	51.1%	0.52	7.7%	17.8%
	57	13	9	6000	105	4	2000	20	13.00	8.91	105.10	4.12	29.45	3.48	53.01	20.88	61.0%	0.50	8.2%	16.6%
	58	13	9	6000	75	8	2000	20	13.05	8.96	75.10	8.06	24.45	5.24	35.85	20.86	41.5%	0.55	6.1%	17.0%
	59	13	9	6000	90	8	2000	20	13.08	9.07	89.88	7.78	26.90	4.58	44.75	22.21	49.5%	0.51	7.4%	17.6%
	60	13	9	6000	105	8	2000	20	13.13	8.98	104.66	8.12	29.29	3.70	52.95	24.45	58.8%	0.49	8.4%	17.4%
	61	13	9	6000	75	12	2000	20	13.02	8.99	75.23	11.94	23.76	5.38	38.79	24.22	40.2%	0.52	5.0%	14.4%
	62	13	9	6000	90	12	2000	20	13.09	9.03	90.14	11.99	26.53	4.78	45.72	26.12	47.1%	0.48	8.1%	19.8%
	63	13	9	6000	105	12	2000	20	13.02	8.96	104.89	12.05	29.12	3.86	53.68	28.29	56.9%	0.47	9.6%	19.9%
	64	13	9	6000	75	16	2000	20	13.17	9.05	75.22	16.12	23.46	5.62	40.98	27.55	37.9%	0.50	5.0%	15.0%
	65	13	9	6000	90	16	2000	20	13.25	9.12	89.90	16.25	26.27	4.96	47.30	29.85	45.6%	0.46	7.4%	18.9%
	66	13	9	6000	105	16	2000	20	13.18	9.08	105.80	16.05	28.92	4.13	54.61	31.96	54.5%	0.44	9.5%	20.4%
	67	13	9	6000	75	20	2000	20	12.88	9.05	74.64	20.67	22.70	5.74	43.49	31.36	36.6%	0.48	4.5%	14.0%
	68	13	9	6000	90	20	2000	20	12.95	9.07	90.68	20.25	25.60	5.11	48.92	33.38	43.7%	0.43	7.9%	20.5%
	69	13	9	6000	105	20	2000	20	13.01	9.01	105.72	20.03	28.22	4.24	55.24	35.88	52.9%	0.43	9.4%	20.6%
	70	13	9	6000	75	24	2000	20	13.02	9.04	74.23	23.99	22.17	5.88	44.51	34.44	35.0%	0.46	3.7%	11.8%
	71	13	9	6000	90	24	2000	20	13.09	9.05	89.74	23.88	25.35	5.17	49.01	36.93	42.9%	0.43	7.4%	19.5%
	72	13	9	6000	105	24	2000	20	13.17	9.03	105.50	23.51	28.15	4.47	55.46	39.13	50.5%	0.41	10.2%	22.9%
<i>Changing air flowrate</i>																				
73	6	4	6000	75	4	2000	20	5.90	3.90	75.10	4.00	15.10	0.88	43.70	14.20	77.4%	0.45	10.7%	17.9%	
	74	6	4	6000	90	4	2000	20	5.98	4.17	89.80	4.06	17.36	0.75	51.88	15.50	82.0%	0.39	17.4%	24.8%
	75	6	4	6000	105	4	2000	20	5.97	4.05	103.22	3.87	18.83	0.60	61.70	15.05	85.2%	0.33	26.4%	32.9%
	76	6	4	5500	75	4	1833	20	6.16	4.05	75.15	4.37	16.47	0.79	42.68	14.35	80.5%	0.48	13.4%	20.9%
	77	6	4	5500	90	4	1833	20	6.05	4.01	90.12	4.03	18.06	0.56	52.52	14.92	86.0%	0.39	21.2%	28.2%
	78	6	4	5500	105	4	1833	20	6.07	4.12	104.89	4.23	19.17	0.44	62.97	15.39	89.3%	0.34	23.9%	29.8%
	79	6	4	5000	75	4	1667	20	6.02	3.97	74.85	4.02	17.02	0.73	40.32	14.30	81.6%	0.48	18.3%	26.3%
	80	6	4	5000	90	4	1667	20	5.88	4.02	91.23	4.05	18.66	0.46	50.86	15.24	88.6%	0.40	24.5%	30.4%
	81	6	4	5000	105	4	1667	20	6.23	3.98	104.12	4.07	19.42	0.27	61.92	15.74	93.2%	0.35	24.3%	29.7%
	82	6	4	4500	75	4	1500	20	6.21	4.09	74.64	4.02	17.71	0.64	38.63	14.95	84.4%	0.51	17.6%	25.0%
	83	6	4	4500	90	4	1500	20	6.19	4.09	90.17	4.26	19.17	0.32	50.21	15.86	92.2%	0.43	21.7%	27.4%
	84	6	4	4500	105	4	1500	20	6.17	4.30	105.10	4.11	19.88	0.15	62.42	16.39	96.5%	0.38	19.8%	24.3%

15 °C, 0.88 g/kg, realizing deep dehumidification under the regeneration temperature of 75 °C. Table 4 evaluates the energy performance of the designed deep dehumidification system, and it can achieve an overall COP_e of 1.86, where COP_e is defined by the dehumidification capacity of the system in relation to the overall electric consumption of the system.

5. Conclusions

This study conducted experiments to investigate the actual dehumidification performance of the desiccant wheel system under the conditions of deep dehumidification. Based on the results, the differences between low humidity and normal humidity dehumidification processes are analyzed. Moreover, the sensitivity to the process and regeneration parameters is investigated and the thermodynamic effectiveness of the desiccant wheel dehumidification system is addressed. The main conclusions are as follows:

- (1) When $\omega_{r,in} = 4 \text{ g/kg}$, the desiccant wheel can effectively remove the moisture of the process air from 6 °C and 4 g/kg to less than 1 g/kg under $t_{r,in} = 75 \sim 105 \text{ }^\circ\text{C}$, with the RDC of the desiccant wheel ranging from 77.4% to 85.2% and DCOP ranging from 0.45 to 0.33.
- (2) The reduction of inlet temperature and humidity ratio of process air, the rise of inlet temperature of regeneration air, as well as the decrease of inlet humidity ratio of regeneration air can improve the dehumidification performance of the desiccant wheel to produce dehumidified air with low humidity.
- (3) The change of regeneration temperature as well as the RDC shows higher sensitivity to improve the dehumidification performance of the desiccant wheel under higher regeneration humidity. The sensitivity of dehumidification performance varying with regeneration humidity is reduced when the desiccant wheel is operated at high regeneration temperature, and the RDC of the system exhibits high independence of the variation of regeneration humidity.
- (4) η_h and η_t of the desiccant wheel dehumidification process are positively correlated and can be involved within a parallelogram range with the change of inlet air parameters. The deep dehumidification process has a significant higher thermodynamic deviation caused by irreversible heat loss. With the rise of regeneration temperature, greater heat loss occurs in the heating process, and both η_h and η_t significantly increase.
- (5) The desiccant wheel can be applied as the final stage of the cascading deep dehumidification system to dehumidify the hot and humid air to the depth of less than 1 g/kg while achieving considerable COP_e and having high application potential.

CRediT authorship contribution statement

Zhiyao Ma: Data curation, Investigation, Formal analysis, Writing – original draft. **Xiaohua Liu:** Conceptualization, Methodology, Supervision. **Tao Zhang:** Investigation, Writing – review & editing.

Declaration of Competing Interest

The authors declare that they have no known competing financial interests or personal relationships that could have appeared to influence the work reported in this paper.

Data availability

Data will be made available on request.

Acknowledgments

This research was supported by the National Key Research Program of China (No. 2019YFF0301504).

Appendix A

The desiccant wheel had a diameter of 0.8 m and a thickness of 0.2 m. The core honeycomb was made of the metal of Aluminum and the desiccant coating on the honeycomb is silica gel. The detailed information of the desiccant wheel and the dehumidification system were listed in Table A1 and Fig. A1. Three quarters of the facial area of the desiccant wheel are used for the dehumidification process, and one quarter of that is used for the regeneration process. The temperature and relative humidity of the air was measured in the inlet and the outlet air ducts of the desiccant wheel, where the air state was fully mixed. The temperature and humidity meter (TJHY WWSZY-1) has a measurement accuracy of $\pm 0.3 \text{ }^\circ\text{C}$ and $\pm 2\%$. The outlet process air state was also examined by the dew point meter (DM70) with a measurement accuracy of $\pm 2 \text{ }^\circ\text{C}$. The difference of the outlet process air humidity ratio measured by TJHY WWSZY-1 and DM70 was within $\pm 0.1 \text{ g/kg}$, so the measurement error was within $\pm 10\%$ for the air humidity ratio of 1.0 g/kg, and it can be viewed as the valid result. The air flow rate of the measurement was controlled by the constant air flow damper operated based on the pressure difference, and it was examined by the anemometer in long lengths of straight ducts of the device. The air flow rate was strictly measured by multiple times in the experiment. All the measurement instruments have been calibrated within two weeks before the experiment.

Appendix B

The summary of full test conditions was listed in Table B1 as follows.

References

- [1] C.K. Chang, L. Lin, S.C. Hu, B.R. Fu, J.S. Hsu, Various energy-saving approaches to a TFT-LCD panel fab, *Sustainability* 8 (2016) 907.
- [2] K. Nagaya, Y. Li, Z. Jin, M. Fukumuro, Y. Ando, A. Akaishi, Low-temperature desiccant-based food drying system with airflow and temperature control, *J. Food Eng.* 75(1) (2006) 71–77.
- [3] W.C. Federation. WCF Curling Ice Requirements[OL], 2014.
- [4] S. Ahmed, P.A. Melson, W.D. Dees, Study of a dry room in a battery manufacturing plant using a process model, *J. Power Sources* 326 (2016) 490–497.
- [5] C.F. Chien, J.T. Peng, H.C. Yu, Building energy saving performance indices for cleaner semiconductor manufacturing and an empirical study, *Comput. Ind. Eng.* 99 (2016) 448–457.
- [6] Z. Ma, X. Liu, T. Zhang, Measurement and optimization on the energy consumption of fans in semiconductor cleanrooms, *Build. Environ.* 197 (2021), 107842.
- [7] M.G.L.C. Loomans, P.C.A. Molenaar, H.S.M. Kort, P.H.J. Joosten, Energy demand reduction in pharmaceutical cleanrooms through optimization of ventilation, *Energy Build.*, 202 (2019) 109346.
- [8] D.B. Jani, M. Mishra, P.K. Sahoo, A critical review on solid desiccant-based hybrid cooling systems, *Int. J. Air-condition. Refrig.* 25(3) (2017) 173002.
- [9] P. Vivekh, M. Kumja, D.T. Bui, K.J. Chua, Recent developments in solid desiccant coated heat exchangers – A review, *Appl. Energy* 229 (2018) 778–803.
- [10] X.N. Wu, T.S. Ge, Y.J. Dai, R.Z. Wang, Review on substrate of solid desiccant dehumidification system, *Renew. Sustain. Energy Rev.* 82 (2018) 3236–3249.
- [11] K.S. Rambhad, P.V. Walké, D.J. Tidke, Solid desiccant dehumidification and regeneration methods - A review, *Renew. Sustain. Energy Rev.* 59 (2016) 73–83.
- [12] D. La, Y.J. Dai, Y. Li, R.Z. Wang, T.S. Ge, Technical development of rotary desiccant dehumidification and air conditioning: A review, *Renew. Sustain. Energy Rev.* 14 (1) (2010) 130–147.
- [13] S. Yamaguchi, K. Saito, Numerical and experimental performance analysis of rotary desiccant wheels, *Int. J. Heat Mass Transf.* 60 (1) (2013) 51–60.
- [14] A. Zendehboudi, H. Esmaili, Effect of supply/regeneration section area ratio on the performance of desiccant wheels in hot and humid climates: an experimental investigation, *Heat Mass Transf.* 52 (6) (2016) 1175–1181.
- [15] D.A. Saputra, Y. Osaka, T. Tsujiguchi, M. Haruki, M. Kumita, A. Kodama, Experimental investigation of desiccant wheel dehumidification control method for changes in regeneration heat input, *Energy* 205 (2020), 118109.
- [16] R. Tu, X.H. Liu, Y. Jiang, F. Ma, Influence of the number of stages on the heat source temperature of desiccant wheel dehumidification systems using exergy analysis, *Energy* 85 (2015) 379–391.

- [17] T.S. Ge, Y.J. Dai, R.Z. Wang, Y. Li, Performance of two-stage rotary desiccant cooling system with different regeneration temperatures, *Energy* 80 (2015) 556–566.
- [18] Y. Liu, Y. Chen, D. Wang, J. Liu, L. Li, X. Luo, et al., Performance evaluation of a hybrid solar powered rotary desiccant wheel air conditioning system for low latitude isolated islands, *Energ. Buildings* 224 (110208) (2020).
- [19] C.R. Ruivo, G. Angrisani, The effectiveness method to predict the behaviour of a desiccant wheel: An attempt of experimental validation, *Appl. Therm. Eng.* 71 (2) (2014) 643–651.
- [20] G. Angrisani, C. Roselli, M. Sasso, Experimental assessment of the energy performance of a hybrid desiccant cooling system and comparison with other air-conditioning technologies, *Appl. Energy* 138 (2015) 533–545.
- [21] M. Gadalla, M. Saghafifar, Performance assessment and transient optimization of air precooling in multi-stage solid desiccant air conditioning systems, *Energ. Convers. Manage.* 119 (2016) 187–202.
- [22] H. Caliskan, D.Y. Lee, H. Hong, Enhanced thermodynamic assessments of the novel desiccant air cooling system for sustainable energy future, *J. Clean. Prod.* 211 (2019) 213–221.
- [23] T.S. Ge, F. Ziegler, R.Z. Wang, H. Wang, Performance comparison between a solar driven rotary desiccant cooling system and conventional vapor compression system (performance study of desiccant cooling), *Appl. Therm. Eng.* 30 (6–7) (2010) 724–731.
- [24] A.E. Kabeel, Solar powered air conditioning system using rotary honeycomb desiccant wheel, *Renew. Energy* 32 (11) (2007) 1842–1857.
- [25] Baniyounes AM, Rasul MG, Khan MMK, Experimental assessment of a solar desiccant cooling system for an institutional building in subtropical Queens- land, Australia. *Energy and Buildings*. 62 (2013) 78–86.
- [26] Subramanyam N, Maiya MP, Murthy SS, Application of desiccant wheel to control humidity in air-conditioning systems, *Appl. Therm. Eng.* 24 (17–18) (2004) 2777–2788.
- [27] Guan B, Ma Z, Wang X, Liu X, Zhang T, A novel air-conditioning system with cascading desiccant wheel and liquid desiccant dehumidifier for low-humidity industrial environments, *Energy and Buildings*. 2022;274:112455.
- [28] M.H. Mahmood, M. Sultan, T. Miyazaki, Experimental evaluation of desiccant dehumidification and air-conditioning system for energy-efficient storage of dried fruits, *Build. Serv. Eng. Res. Technol.* 41 (4) (2020) 454–465.
- [29] S. Ahmed, P.A. Nelson, D.W. Dees, Study of a dry room in a battery manufacturing plant using a process model, *J. Power Sources* 326 (2016) 490–497.
- [30] B. Guan, T. Zhang, X. Liu, On-site performance investigation of a desiccant wheel deep-dehumidification system applied in lithium battery manufacturing plant, *Energ. Buildings* 232 (2021), 110659.
- [31] Q. Chen, J.R. Jones, R.H. Archer, A dehumidification process with cascading desiccant wheels to produce air with dew point below 0 °C, *Appl. Therm. Eng.* 148 (2019) 78–86.
- [32] B. Guan, X. Liu, X. Wang, T. Zhang, Z. Zhou, Regeneration energy analysis on desiccant wheel system in curling arena for the Winter Olympics, *Build. Environ.* 214 (2022), 108960.
- [33] B. Guan, X. Liu, T. Zhang, Z. Ma, L. Chen, X. Chen, Experimental and numerical investigation of a novel hybrid deep-dehumidification system using liquid desiccant, *Energ. Convers. Manage.* 192 (2019) 396–411.
- [34] B. Su, W. Qu, W. Han, H. Jin, Feasibility of a hybrid photovoltaic/thermal and liquid desiccant system for deep dehumidification, *Energ. Convers. Manage.* 163 (2018) 457–467.
- [35] B. Guan, T. Zhang, L. Jun, X. Liu, Exergy analysis and performance improvement of liquid-desiccant deep-dehumidification system: An engineering case study, *Energy* 196 (2020), 117122.